Supporting Information for

Kinetics, isotherms and adsorption-desorption behavior of phosphorous from aqueous solution using zirconium-iron and iron modified biosolid biochars

Md. Aminur Rahman*[1,2,3], Dane Lamb*[2,4], Anitha Kunhikrishnan[1,2], Mohammad Mahmudur Rahman[1]

[1]Global Centre for Environmental Remediation (GCER), College of Engineering, Science and Environment, The University of Newcastle, Callaghan, NSW 2308, Australia

[2]Cooperative Research Centre for High Performance Soils, Callaghan, NSW 2308, Australia

[3]Department of Public Health Engineering (DPHE), Zonal Laboratory, Khulna-9100, Bangladesh

[4]Chemical and Environmental Engineering, School of Engineering, RMIT University, Melbourne, Victoria, 3000, Australia

Corresponding Author: Md. Aminur Rahman (md.aminur.rahman@uon.edu.au) and Dr. Dane Lamb (dane.lamb@rmit.edu.au)

University of Newcastle, ATC Building, University Drive, Callaghan NSW 2308, Australia

S1. BET-N_2 surface area

Specific surface area (SSA) of biochar samples (<2 mm) were measured with nitrogen (N_2) adsorption isotherms under liquid N_2 (-196 °C) by a Surface Area and Porosity Analyzer (TristarII 3020, Micromeritics, USA). Biochar samples were degassed overnight at 60 °C under at 2 Torr before N_2 adsorption (micromeritics VacPrep 061 Sample Degas System). The BET (Brunauer-Emmett-Teller) [1] equation were used to calculate the surface area of the biochar samples. BET and Langmuir adsorption isotherms were generated to determine the single-point surface area. Pore volume and pore diameter of all biochars were measured using a gas adsorption analyzer by BET method. The mean diameter of the biochar was measured using a Zeta plus particle size analyzer (NanoPlus HD, USA). The lower detection range of the particle size of the analyzer is 2 nm to 3 μm.

S 2. Zeta potential and particle size measurement

Electrophoretic mobility of biochar, namely zeta potential (ZP), can be used to evaluate surface charge properties of particulate systems. ZP is the electrical potential of a sliding plane between the stern and diffuse layers of colloidal particles. [2, 3] ZP was determined for each biochar samples using a Zeta-Analyzer (NanoPlus HD, Micromeritics, USA) following the electrophoretic light scattering method. All samples were dried and passed through a No. 200 sieve prior to measurement. A solution containing 0.01 g biochar in 50 mL (0.02%, w/V) $NaNO_3$ (0.01 M) was prepared. A small amount of the solution was placed into the cell. The velocity of particles moving toward a positively charged electrode, which is determined to compute the ZP of each sample using Zeta-Meter.

The particle size of biochars were determined following the dynamic light scattering method by using the nano particle analyzer (NanoPlus HD, Particulate systems, Micromeritics, USA). In this method, the fluctuations in time of scattered light from particles in Brownian motion were measured. Since the particles in Brownian motion moved randomly, the scattered intensity fluctuations are also random. Thus, the fluctuations occurred rapidly for smaller moving particles and more slowly for larger and slower moving particles. Therefore, the fluctuations of the scattered light were analyzed using the autocorrelation function. Before measuring the particle size of biochar sample, the instrument was calibrated using the aqueous suspension of standard polystyrene latex (mean diameter 110nm ± 3%) sourced from Otsuka

Electronics Co., Ltd. This measurement was taken in triplicate and average values were recorder for each biochar samples.

S 3. Isoelectric point

The pH at which the net charge of a solid surface is zero, is referred to as isoelectric point or point of zero charge (pH_{PZC}), which is one of the most important parameters used to describe variable-charge [4, 5]. A Zeta-Analyzer (NanoPlus HD, Micromeritics, USA) was used to determine the PZC, where 0.02 g (0.02 % w/V) biochar was taken in a centrifuge tube using $NaNO_3$ (0.01 M) as a background electrolyte. The pH of biochar suspension was adjusted to 1.0–11using 0.1 M HNO_3 and/or NaOH and then kept in a rotary shaker for 24 hours. The samples were placed in a sonicator for 15 minutes after being reached to equilibrium and then biochar suspension was injected into the Zeta-analyzer. After successful calibrating the instrument, the PZC was determined from plotting the pH vs zeta potential (where intersects the curve).

S 4. pH and electrical conductivity measurement

pH and electrical conductivity (EC) of unmodified and modified biochars were measured in both water and $CaCl_2$ maintaining a 1:20 biochar to solution ratio (w/V). pH values were measured using a pH meter (Mettler Toledo FF28, Australia), supplied with a combined electrode, calibrated using commercial pH 4.01, 7.01 and 9.23 buffers. All analysis were performed in triplicate and the average values were recorded. Results were shown in **Table 1.**

S 5. Cation exchange capacity (CEC)

Surface charge properties of biochars were determined by CEC and electrophoretic mobility property of biochars. Cation exchange capacity (CEC) is an indicator of abundance charge on the surface of a material, which can be balanced by exchangeable cations.[6-8] In this study, CEC of biochar was determined by $BaCl_2$ compulsive exchange modified method as described by Gillman and Sumpter (1986) [9]. Results are inserter in **Table 1**.

S 6. Determination of C, N and S

Air-dried biochars (at 80 °C) were placed into glass vials. The contents of C, N, and S (wt %) were determined for each biochar samples by a CNS analyzer using a LECO TruMac operated in CHN mode. Results were tabulated in **Table S2.**

S 7. Major cations analysis

Determination of As and other major metals such as Na, K, Mg, Ca, Fe, Al, and P of biochars were extracted by microwave digestion in aqua regia following USEPA 3051 40 method. An inductively coupled plasma optical-emission spectrometer (ICP-OES, PerkinElmer Avio 200, USA) setting with dual view (axial and radial) were used to determine the concentration of As and other major metals.

S 8. Sorption kinetic models

The experimental results from kinetic studies were fitted using the following models:

The pseudo-first-order kinetic model [10]:

$$\log(q_e - q_t) = \log q_e - [k_1/2.303]t \qquad \ldots\ldots\ldots\ldots \text{(Eq. S1)}$$

Where k_1 (h^{-1}) is the pseudo-first-order rate constant and q_e (mg g^{-1}) is the P adsorption capacity at equilibrium, and q_t (mg g^{-1}) is the adsorbed amount of P after time t (h). The first-order rate constant (k_1) and q_e were calculated from the slope and intercept of plots of $\log(q_e - q_t)$ vs t.

The pseudo-second-order kinetic model [11]:

$$t/q_t = 1/k_2 . 1/q_e^2 + t/q_e \qquad \ldots\ldots\ldots\ldots\ldots\ldots \text{(Eq. S2)}$$

Where k_2 is the pseudo-second-order rate constant (g mg^{-1} h^{-1}). q_e and q_t described the amount of adsorbed P (mg g^{-1}) at equilibrium and at any time after t (h). The parameters q_e and k_2 were calculated from the slope and intercept of pseudo second order kinetics plot of t/q_t Vs t.

The pseudo-second order model is commonly used to describe adsorption kinetics in which chemical adsorption controls the adsorption rate and in which the number of active adsorption sites on the biochar surface and the number of adsorbate ions in the liquid phase together determines the sorption capacity [12]. The formation of chemical bond between adsorbate and number of adsorbing sites is the rate-limiting step [13].

Elovich model [14] kinetic model assumes that solid adsorbent surface is generically heterogeneous and no lateral interaction takes place between the adsorbed solute. Linearized form of Elovich model is represented by the following expression (Eq. S3):

$$q_t = \beta \ln(\alpha\beta) + (\ln t) \quad \text{.....(Eq. S3)}$$

where q_t is the amount of adsorbed P by biochars at any time t, α is the adsorption kinetic at the beginning (mg g^{-1} h^{-1}), and β is the adsorption constant related to the extent of surface coverage and the activation energy for chemisorption during the experiments (g mg^{-1}). The constants α and β were obtained from the slope and intercept of the linear plot of qt vs lnt.

The intraparticle diffusion model [15] can be expressed using equation (Eq. S4).

$$q_t = k_{id}\, t^{1/2} + C \quad \text{.....(Eq. S4)}$$

where, q_t is the P adsorption capacity at any time t and k_{id} is the intraparticle diffusion rate constant (mg/g $h^{1/2}$) and C (mg g^{-1}) is the constant which gives an impression of the film thickness of the boundary layer indicating the larger the intercept, the greater the boundary layer effect [16]. The slope and intercept of the linear plot of q_t Vs $t^{1/2}$ was used to calculate K_{id} and C. If the plot of q_t Vs $t^{1/2}$ is linear and passes through the origin, i.e. C=0, then the adsorption process is considered to be only controlled by the intraparticle diffusion [17] and the multi-linear plot is attributed to the process controlled by more than one mechanism [18].

S 9. Sorption isotherm models

The Langmuir model (monolayer model) is described by the Eq. S5 [19]:

$$q_e = q_m C_e K_L/(1 + C_e K_L) \quad \text{.....(Eq. S5)}$$

Where q_e is the adsorbed amount of P (mg g^{-1}) in equilibrium at solid phase, q_m is the maximum P adsorption capacity (mg g^{-1}) by biochars, which represents the complete monolayer coverage of adsorbent with adsorbate. C_e (mg L^{-1}) is the equilibrium P concentration and K_L is an

equilibrium constant (L mg^{-1}) related to binding strength. The constants are calculated from slope and intercept of the linear plots of C_e/q_e versus C_e, respectively. The Langmuir isotherm can also be explained by separation factor (R_L) using the equation (Eq. S6).

$$R_L = 1/(1+K_L C_0) \quad \text{.....(Eq. S6)}$$

Where C_0 (mg L^{-1}) is the initial P concentration. There are four probabilities for the R_L value; (i) $0<R_L<1$, for favourable sorption, (ii) $R_L>1$, for unfavourable sorption, (iii) $R_L = 1$, for linear sorption, and (iv) $R_L = 0$, for irreversible sorption.

The Freundlich equation (nonlinear model) is an empirical adsorption model which is expressed as the following equation (Eq. S7) [20].

$$q_e = K_F C_e^{1/n} \quad \text{.....(Eq. S7)}$$

Where q_e is the adsorbed amount of P (mg g^{-1}) at equilibrium on solid phase and C_e (mg L^{-1}) is the equilibrium P concentration. K_F is a Freundlich affinity coefficient related to the measure of the adsorption capacity and n is a Freundlich exponential coefficient measure of the adsorption intensity. Linear form of Freundlich equation is expressed by equation (Eq. S8).

$$\log q_e = 1/n \log C_e + \log K_f \quad \text{.....(Eq. S8)}$$

The Freundlich isotherm is based on the assumption of multilayer sorption on an energetically heterogeneous surface and can be used to describe the chemisorption process [21, 22].

The Temkin isotherm is applied using the following equation (Eq. S9).

$$q_e = B\ln A + B\ln Ce \quad \text{.....(Eq. S9)}$$

Where q_e is the amount of adsorbed P at equilibrium (mg g^{-1}); C_e is the concentration of P in solution at equilibrium (mg L^{-1}). B is a constant related to the heat of adsorption which is represented by the expression B= RT/b, b is the Temkin constant (J mol^{-1}), T is the absolute

temperature (K), R is the gas constant (8.314 J/mol.K), and A is the Temkin isotherm constant (L g^{-1}). The constants B and A were calculated from the plot of q_e Vs $\ln C_e$.

The Temkin isotherm assumes linear rather than logarithm decrease of heat of adsorption while ignoring extremely low and very high concentration. It also assumes uniform distribution of bonding energy up to some maximum bonding energy.

Table S1. Zeta potential of pristine and modified biochars

	Zeta potential (mV)			
pH	BC	Zr-BC	Zr-FeBC	Fe-BC
2	+5.21	+17.37	+25.02	+12.23
3	+2.63	+21.91	+21.15	+16.21
4	-2.03	-5.12	+15.43	+4.66
5	-7.65	-13.32	+9.98	-7.46
6	-10.28	-20.28	-4.78	-6.66
7	-13.54	-31.26	-13.79	-6.86
8	-14.73	-35.54	-12.21	-7.05
9	-17.36	-27.28	-16.45	-10.13
10	-20.59	-25.87	-19.72	-12.57
11	-24.21	-31.55	-25.68	-15.36

Table S2. Total elemental composition of biochars

Biochar	C (%)	N (%)	S (%)	Concentration (mg g^{-1})						
				Na	K	Mg	Ca	Fe	Al	P
BC	22.88	3.60	1.12	1.99	4.24	7.76	22.97	100.69	29.65	54.86
Zr-BC	20.71	3.10	1.11	26.99	2.83	8.82	18.84	79.12	20.37	26.83
Zr-FeBC	17.88	2.76	0.85	27.18	1.59	4.35	11.88	238.82	17.32	6.12
Fe-BC	22.96	3.47	1.67	12.75	2.34	4.05	15.04	228.17	22.10	7.86

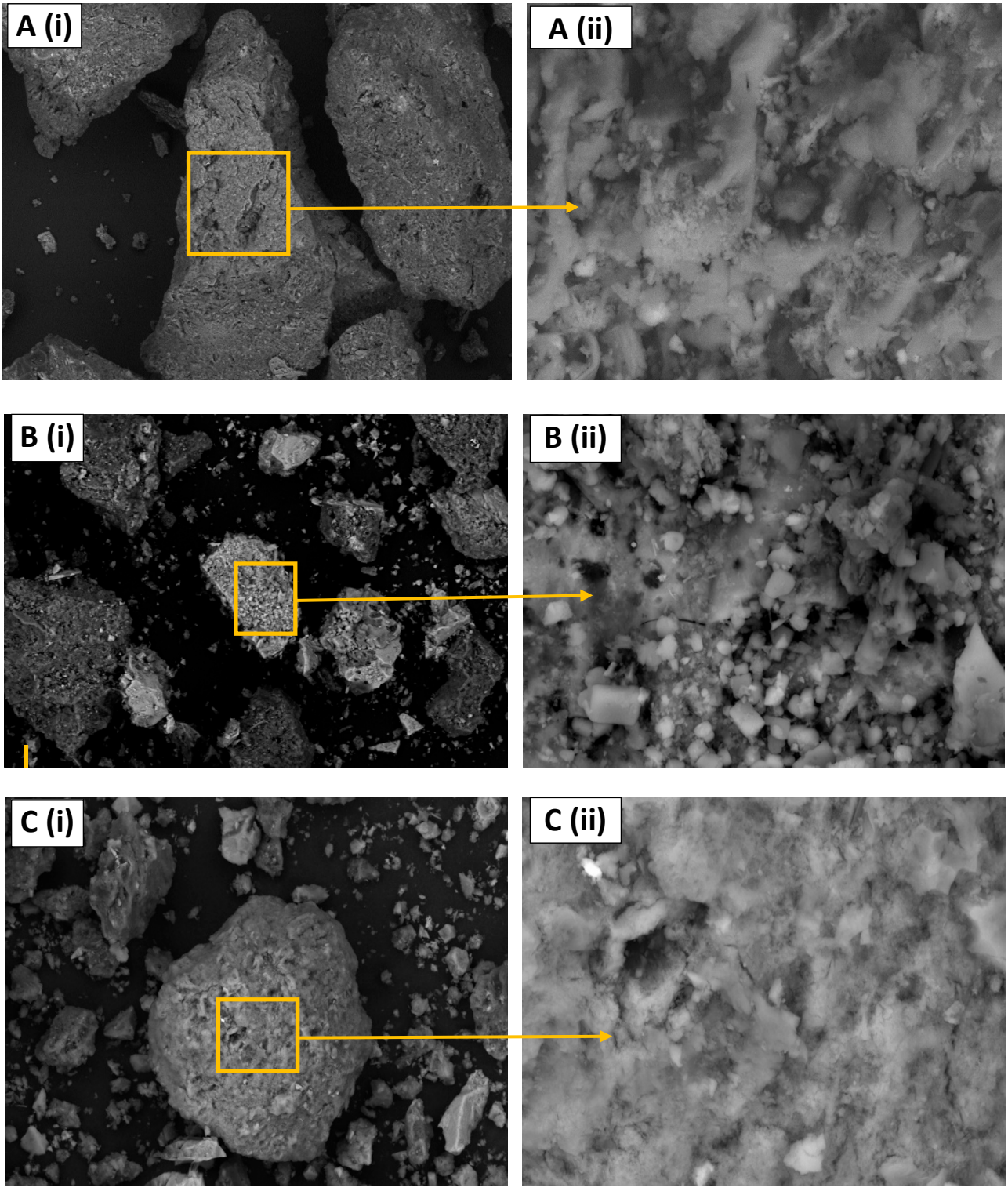

Figure S1. SEM images: A(i-ii) for BC, B(i-ii) for Zr-FeBC and C(i-ii) for Fe-BC [23]

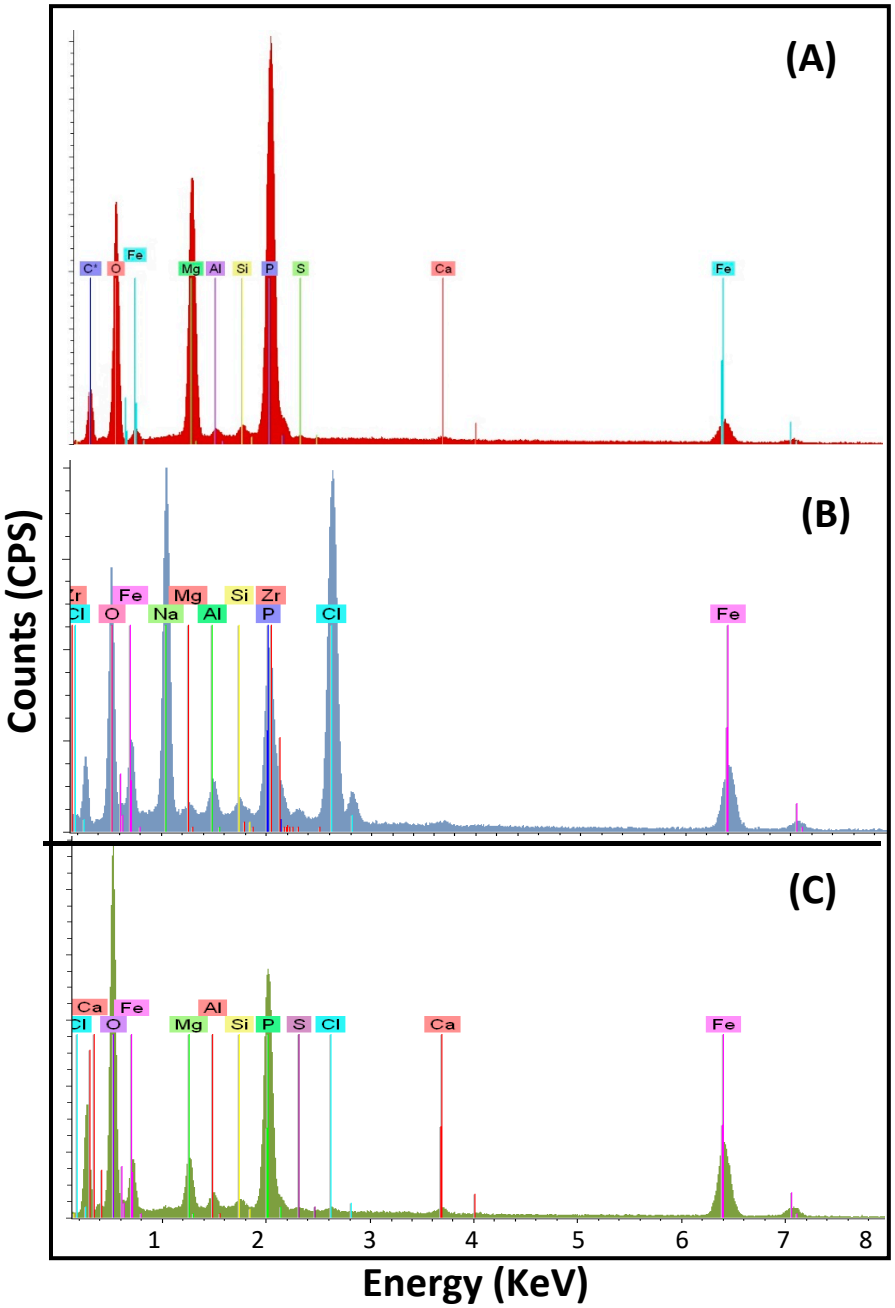

Figure S2. SEM-EDS spectra: (A) for BC, (B) for Zr-FeBC and (C) for Fe-BC [23]

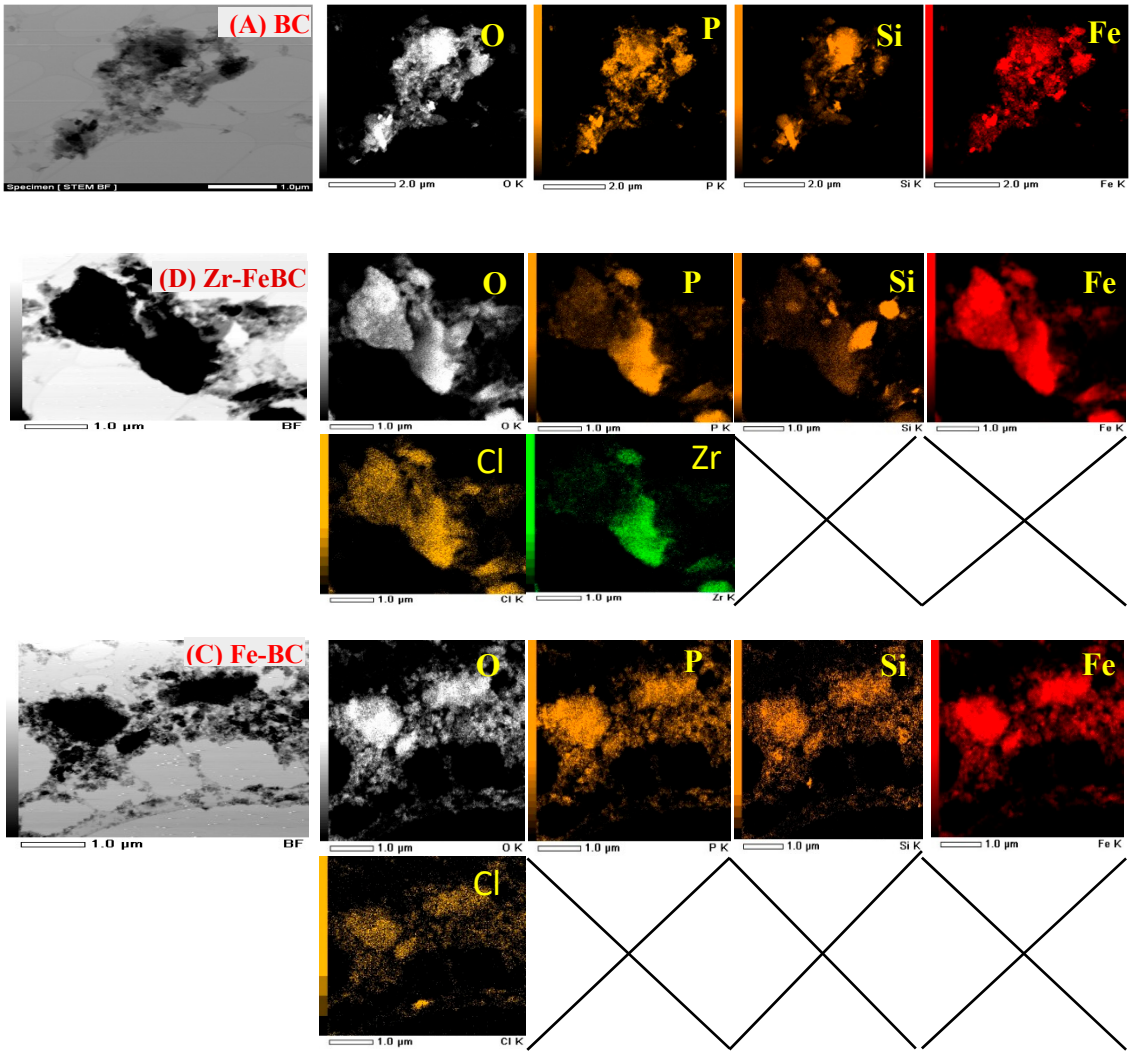

Figure S3. TEM elemental images of (A) BC, (B) Zr-FeBC, and (C) Fe-BC

S 9. Reference

[1] S. Brunauer, P.H. Emmett, E. Teller, Adsorption of gases in multimolecular layers, Journal of the American chemical society, 60 (1938) 309-319.
[2] C. Appel, L.Q. Ma, R.D. Rhue, E. Kennelley, Point of zero charge determination in soils and minerals via traditional methods and detection of electroacoustic mobility, Geoderma, 113 (2003) 77-93.
[3] S. Jiang, T.A. Nguyen, V. Rudolph, H. Yang, D. Zhang, Y.S. Ok, L. Huang, Characterization of hard- and softwood biochars pyrolyzed at high temperature, Environmental geochemistry and health, 39 (2017) 403-415.

[4] F.I. Morais, A. Page, L. Lund, The Effect of pH, Salt Concentration, and Nature of Electrolytes on the Charge Characteristics of Brazilian Tropical Soils 1, Soil Science Society of America Journal, 40 (1976) 521-527.
[5] G.A. Parks, P.D. Bruyn, The zero point of charge of oxides1, The Journal of Physical Chemistry, 66 (1962) 967-973.
[6] J. Jiang, R.-k. Xu, T.-y. Jiang, Z. Li, Immobilization of Cu (II), Pb (II) and Cd (II) by the addition of rice straw derived biochar to a simulated polluted Ultisol, Journal of hazardous materials, 229 (2012) 145-150.
[7] A. Mukherjee, A. Zimmerman, W. Harris, Surface chemistry variations among a series of laboratory-produced biochars, Geoderma, 163 (2011) 247-255.
[8] L. Zhao, X. Cao, W. Zheng, Q. Wang, F. Yang, Endogenous minerals have influences on surface electrochemistry and ion exchange properties of biochar, Chemosphere, 136 (2015) 133-139.
[9] G. Gillman, E. Sumpter, Modification to the compulsive exchange method for measuring exchange characteristics of soils, Soil Research, 24 (1986) 61-66.
[10] Y. Ho, A review of potentially low cost adsorbent for heavy metals, Scientometrics, 59 (2004) 171-177.
[11] Y.-S. Ho, Review of second-order models for adsorption systems, Journal of hazardous materials, 136 (2006) 681-689.
[12] T. Li, X. Su, X. Yu, H. Song, Y. Zhu, Y. Zhang, La (OH) 3-modified magnetic pineapple biochar as novel adsorbents for efficient phosphate removal, Bioresource technology, 263 (2018) 207-213.
[13] Y.-S. Ho, G. McKay, Pseudo-second order model for sorption processes, Process biochemistry, 34 (1999) 451-465.
[14] J. Zeldowitsch, Adsorption site energy distribution, Acta phys. chim. URSS, 1 (1934) 961-973.
[15] W.J. Weber, J.C. Morris, Kinetics of adsorption on carbon from solution, Journal of the Sanitary Engineering Division, 89 (1963) 31-60.
[16] N. Kannan, M.M. Sundaram, Kinetics and mechanism of removal of methylene blue by adsorption on various carbons—a comparative study, Dyes and pigments, 51 (2001) 25-40.
[17] S. Chen, Q. Yue, B. Gao, Q. Li, X. Xu, Removal of Cr (VI) from aqueous solution using modified corn stalks: Characteristic, equilibrium, kinetic and thermodynamic study, Chemical Engineering Journal, 168 (2011) 909-917.
[18] C.-P. Chio, M.-C. Lin, C.-M. Liao, Low-cost farmed shrimp shells could remove arsenic from solutions kinetically, Journal of hazardous materials, 171 (2009) 859-864.
[19] I. Langmuir, The constitution and fundamental properties of solids and liquids. Part I. Solids, Journal of the American chemical society, 38 (1916) 2221-2295.
[20] H. Freundlich, Over the adsorption in solution, J. Phys. Chem, 57 (1906) 1100-1107.
[21] A. Sarı, G.n.r. Şahinoğlu, M. Tüzen, Antimony (III) adsorption from aqueous solution using raw perlite and Mn-modified perlite: equilibrium, thermodynamic, and kinetic studies, Industrial & engineering chemistry research, 51 (2012) 6877-6886.
[22] N.K. Niazi, I. Bibi, M. Shahid, Y.S. Ok, S.M. Shaheen, J. Rinklebe, H. Wang, B. Murtaza, E. Islam, M.F. Nawaz, n, Science of the Total Environment, 621 (2018) 1642-1651.
[23] M.A. Rahman, M.M. Rahman, M.M. Bahar, P. Sanderson, D. Lamb, Antimonate sequestration from aqueous solution using zirconium, iron and zirconium-iron modified biochars, Scientific reports, 11 (2021) 1-11.